

## Fluorescent Flippers for Mechanosensitive Membrane Probes

Marta Dal Molin,\* Quentin Verolet, Adai Colom, Romain Letrun, Emmanuel Derivery, Marcos Gonzalez-Gaitan, Eric Vauthey, Aurélien Roux, Naomi Sakai, and Stefan Matile\*

School of Chemistry and Biochemistry, National Centre of Competence in Research (NCCR) Chemical Biology, University of Geneva, Geneva, Switzerland

### Supporting Information

**ABSTRACT:** In this report, “fluorescent flippers” are introduced to create planarizable push–pull probes with the mechanosensitivity and fluorescence lifetime needed for practical use in biology. Twisted push–pull scaffolds with large and bright dithienothiophenes and their *S,S*-dioxides as the first “fluorescent flippers” are shown to report on the lateral organization of lipid bilayers with quantum yields above 80% and lifetimes above 4 ns. Their planarization in liquid-ordered ( $L_o$ ) and solid-ordered ( $S_o$ ) membranes results in red shifts in excitation of up to +80 nm that can be transcribed into red shifts in emission of up to +140 nm by Förster resonance energy transfer (FRET). These unique properties are compatible with multidomain imaging in giant unilamellar vesicles (GUVs) and cells by confocal laser scanning or fluorescence lifetime imaging microscopy. Controls indicate that strong push–pull macrodipoles are important, operational probes do not relocate in response to lateral membrane reorganization, and two flippers are indeed needed to “really swim,” i.e., achieve high mechanosensitivity.

To uncover the secrets of biological membranes, that is, their order, homogeneity, tension, potential, and so on, many inspired approaches to fluorescent probes have been conceived over the years.<sup>1</sup> They explore the usefulness of excited-state polarization (intramolecular charge transfer in push–pull chromophores, solvatochromism, electrochromism),<sup>2</sup> twisted intramolecular charge transfer (TICT),<sup>3</sup> excited-state intramolecular proton transfer (ESIPT),<sup>4</sup> Förster resonance energy transfer (FRET),<sup>5</sup> photoinduced electron transfer (PET),<sup>6</sup> two-photon absorption (TPA),<sup>7</sup> second harmonic generation (SHG),<sup>8</sup> fluorescence lifetime imaging microscopy (FLIM),<sup>9</sup> and  $\lambda$ -ratiometry.<sup>10</sup> Recently, we have introduced the concept of planarizable push–pull probes (Figure 1A).<sup>11</sup> This combination of polarization<sup>1,2,12</sup> and planarization<sup>13</sup> is interesting because it applies lessons from nature<sup>11,12</sup> and promises access to the imaging not only of the lateral organization of biomembranes<sup>2,3,5–8</sup> but also of membrane potentials<sup>1,3–5,7,8,12</sup> and the poorly detectable but biologically important membrane tension.<sup>14</sup> Focusing on ground-state planarization and thus changes in the excitation spectrum,<sup>11</sup> planarizable push–pull probes can be envisioned as complementary to molecular rotors that operate with excited-state deplanarization and, thus, as most other fluorescent probes, with changes in emission or quantum yield.<sup>3,9</sup>

The concept of planarizable push–pull probes has been elaborated with oligothiophenes.<sup>11</sup> Meticulous sculpting with regard to length, donors, acceptors as well as a comprehensive coverage of the quaterthiophene twistome gave probe **1** that could visualize the fluidity of lipid bilayer membranes for the “naked eye” (Figure 1A). Most importantly, it was found that intermediate twisting was ideal, whereas weak twists gave poor shifts because there is little to planarize and strong twists gave poor shifts because planarization became too hard. However, with oligothiophenes,<sup>15</sup> red shifts obtained upon planarization in  $S_o$  lipid bilayers could reach only up to  $\Delta\lambda_{\text{ex}} = +44$  nm, and fluorescence became very weak with increasing twisting. These limitations were attributed to the poor mechanosensitivity of the small thiophene ring and the negligible fluorescence of isolated thiophene monomers in twisted oligomers. To overcome these two limitations, monomers with large surface area and high intrinsic quantum yield would have to be incorporated into the twisted oligomers. In the following, the term “fluorescent flippers” (or swimfins) is used as a “symbol” for such large and bright monomers in twisted oligomers because, although not fully fitting with regard to all aspects, they provide a helpful memorizer that associates correctly with the characteristics of interest (Figure 1B). The previously explored thiophene monomers<sup>11</sup> failed to perform as fluorescent flippers because they do not fluoresce and their surface area is too small to feel the environment well. Here, we introduce dithienothiophenes and their *S,S*-dioxides<sup>16</sup> as the first fluorescent molecular flippers and show that the new push–pull mechanophore **2** provides access to membrane probes with high mechanosensitivity and long fluorescence lifetime.

Flipper probe **2** was designed as follows (Figure 1B). The twist between the dithienothiophene and the dithienothiophene *S,S*-dioxide flipper was induced with two proximal methyl groups. To enhance the push–pull system, the electron-deficient dithienothiophene *S,S*-dioxide was terminated with an aldehyde acceptor, whereas the electron-rich dithienothiophene was terminated with a methylene donor. A negative charge was added at the donor terminus to ensure delivery to and oriented partitioning into lipid bilayer membranes. Fluorophores **4–6** were designed as controls with either reduced macrodipole or one flipper only.

The synthesis of mechanophore **2** is outlined in Scheme 1. Bromothiophene **7** was converted into the dithienothiophene monomer **8** following reported procedures.<sup>16</sup> Vilsmeier formylation afforded the key intermediate **9**. Bromination of

Received: October 17, 2014

Published: January 13, 2015

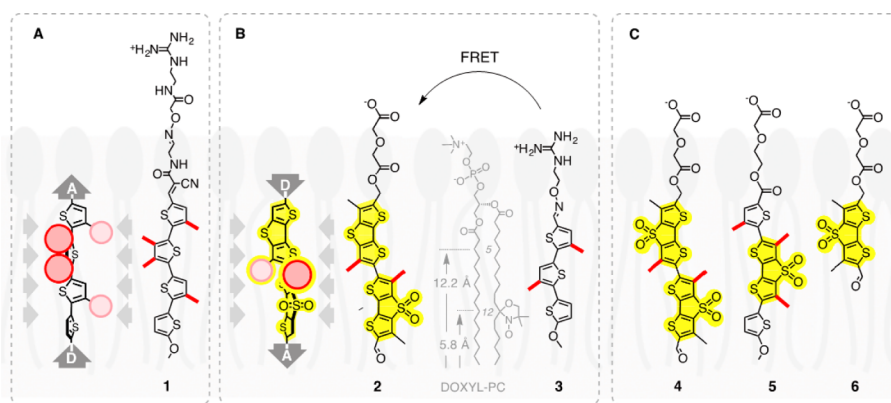
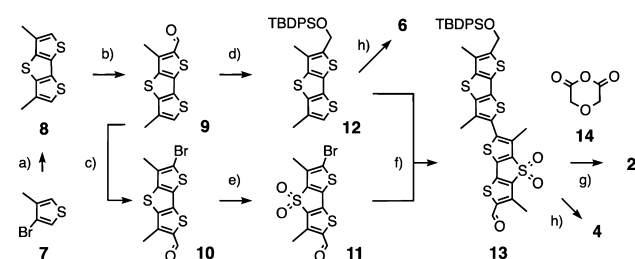


**Figure 1.** (A) Planarizable push–pull probes are conjugated oligomers with electron donors (D) and acceptors (A) at their termini and bulky twist inducers along the scaffold (red circles); their planarization in lipid bilayers is expected to report on membrane order, potential and tension (horizontal gray arrows). (B) Fluorescent flippers, i.e., monomers in twisted push–pull probes with high surface area and fluorescence, are introduced to maximize mechanosensitivity and fluorescence lifetime. Double-flipper probe **2** is shown together with FRET donor **3** (B), push–pull control **4**, single-flipper controls **5** and **6** (C) and original oligothiophene **1** (A).

### Scheme 1<sup>a</sup>



<sup>a</sup>(a) 1.  $\text{S}(\text{SnBu}_3)_2$ ,  $\text{Pd}(\text{PPh}_3)_4$ , toluene, 130 °C, **2**.  $\text{BuLi}$ ,  $\text{CuCl}_2$ ,  $\text{Et}_2\text{O}$ , 0 °C to rt, 64%; (b)  $\text{POCl}_3$ , DMF, 50 °C, 75%; (c) NBS, DMF, 80 °C, 80%; (d) 1.  $\text{NaBH}_4$ , DMF, 2. imidazole, TBDPSCl, DMF, 70%; (e) mCPBA,  $\text{CHCl}_3$ , 40 °C, 65%; (f) 1. LDA,  $\text{Bu}_3\text{SnCl}$ , THF, 2. **11**,  $\text{Pd}(\text{PPh}_3)_4$ , DMF, 46%; (g) 1. TBAF, AcOH, THF, rt, 2. **14**, TEA, THF, 60 °C, 38%; (h) several steps, see Scheme S1.

aldehyde **9** and oxidation of product **10** with mCPBA gave  $S,S$ -dioxide **11**. Reduction of aldehyde **9** followed by silyl protection of the obtained alcohol gave dithienothiophene **12**. Stille coupling of **11** and **12** gave the double flipper **13**, deprotection and esterification with the cyclic anhydride **14** the target probe **2**. Double-flipper control **4** was accessible in a few steps from **13**, single flipper **6** from intermediate **12**, donor **3** and control **5** were prepared similarly (Schemes S2–S4).

The absorption maximum of the push–pull system in flipper probe **2** in chloroform was at  $\lambda_{\text{abs}} = 435$  nm (Figure S5). The emission maximum showed significant solvatochromism from 530 to almost 700 nm (Figure S5). Lippert analysis<sup>11</sup> of the dependence of the Stokes shift on solvent polarity gave a variation of permanent dipole moment upon excitation of  $\Delta\mu = 14$  D (Table S1). In comparison, blue-shifted absorption in chloroform at 418 nm and with  $\Delta\mu = 11$  D weaker solvatochromism confirmed that the push–pull system of **4** is weaker than that of **2**. The fluorescence quantum yield of the push–pull system of **2** in chloroform was  $\phi = 83\%$  (control **4**,  $\phi = 66\%$ ; **5**,  $\phi = 32\%$ ; cf. **1**,  $\phi = 20\%$ <sup>11</sup>). This excellent value compared very well with the reported quantum yields of dithienothiophene  $S,S$ -dioxides<sup>16</sup> and thus confirmed that chromophore twisting does not reduce fluorescence.

Dependent on the nature of the phospholipids used, bilayer membranes undergo a sharp transition from liquid-disordered ( $L_d$ ) or fluid phase to solid-ordered ( $S_o$ ) or gel phase at a

characteristic temperature, the chain-melting temperature  $T_m$ .<sup>1,3,11,17</sup> With increasing concentration of cholesterol, this phase transition disappears, and the mixed membranes exist permanently in the liquid-ordered ( $L_o$ ) phase, which is characterized by short-range orientational order and long-range translational disorder.<sup>17</sup> In multicomponent bilayers, binary mixtures of lipids with cholesterol and beyond,  $L_o$  and  $L_d$  membranes can coexist as immiscible microdomains.<sup>1,3,11</sup> Viscosity and elastic modulus increase from  $L_d$  over  $L_o$  to  $S_o$  phase, whereas lateral diffusion decreases. For example, diffusion coefficients in  $L_o$  are about 3 to 5 times smaller than in  $L_d$  phase.<sup>17</sup> Viscosity increases from 100–300 cP in  $L_d$  to up to 1300 cP in  $S_o$  phase.<sup>3a</sup>

The mechanosensitivity of flipper probe **2** was evaluated in large unilamellar vesicles (LUVs). LUVs composed of DPPC (dipalmitoyl-*sn*-glycero-3-phosphocholine) have a  $S_o$ – $L_d$  transition at 41 °C. The excitation spectrum of 1.0  $\mu\text{M}$  **2** (1.3 mol %) added to  $L_d$  DPPC LUVs at 55 °C showed two maxima at  $\lambda_{\text{ex}} = 453$  nm and  $\lambda_{\text{ex}} = 329$  nm of equal intensity ( $\Delta F_{\text{ex}}^1/F_{\text{ex}}^2 = 0.97$ , Figure 2A, red, solid). The  $\Delta\lambda_{\text{ex}} = +18$  nm from chloroform suggested that flipper probe **2** could already be partially planarized in  $L_d$  DPPC. Cooled down to 25 °C, an intense peak with a flat maximum  $\lambda_{\text{ex}} = 498$ –533 nm emerged, accompanied by a sharper but weaker band at  $\lambda_{\text{ex}} = 352$  nm ( $\Delta F_{\text{ex}}^1/F_{\text{ex}}^2 = 1.48$ , Figure 2A, blue, solid). A red shift of up to  $\Delta\lambda_{\text{ex}} = +80$  nm in response to  $L_d$ – $S_o$  transition, obtained with the first unoptimized flippers, clearly exceeded  $\Delta\lambda_{\text{ex}} = +44$  nm of the best flipper-free probe **1**. This finding supported that increasing surface area in twisted push–pull probes increases mechanosensitivity, as expected from “fluorescent flippers.”

Several control experiments were conceived to probe the validity of these important conclusions. The temperature independence of the excitation maxima of **2** in DOPC (dioleoyl-*sn*-glycero-3-phosphocholine) was important because DOPC membranes are always in  $L_d$  phase (Figure 2A, dotted). Excluding thermochromism, this finding supported that the up to  $\Delta\lambda_{\text{ex}} = +80$  nm found in  $S_o$  DPPC originates indeed from ground-state planarization of the twisted flippers. The concentration independence of the spectroscopic properties, most importantly, excluded contributions from aggregation<sup>13</sup> to the mechanosensitivity of **2** (Figure S4). The insensitivity of the emission maxima of **2** at  $\lambda_{\text{em}} = 600$  nm to temperature, concentration, lipid composition and lateral organization (Figure 2B) supported that

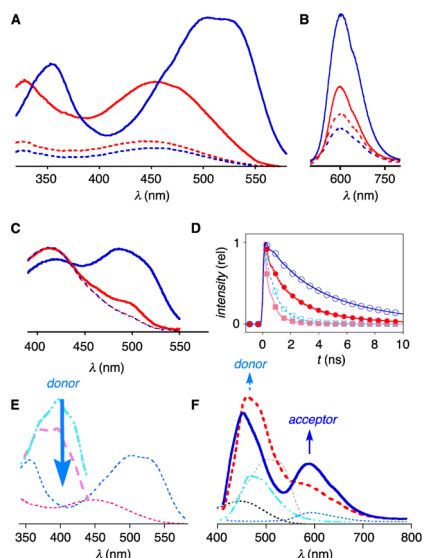


**Figure 2.** (A) Excitation spectra of **2** in DPPC LUVs (solid) and DOPC LUVs (dotted) at 25 °C (blue) and 55 °C (red,  $\lambda_{em} = 600$  nm). (B) Same for emission ( $\lambda_{ex} = 420$  nm). (C) Excitation spectra of **4** in DPPC LUVs (solid) and DOPC LUVs (dotted) at 25 °C (blue) and 55 °C (red,  $\lambda_{em} = 600$  nm). (D) Time-resolved fluorescence decay of **2** (circles) and **1** (squares) in DPPC LUVs (empty) and DOPC LUVs (filled) at 25 °C. (E and F) Transcription of excitation shift to emission shift by FRET. (E) Excitation spectra of donor **3** (dashed,  $\lambda_{em} = 460$  nm) and acceptor **2** (dotted,  $\lambda_{em} = 600$  nm) in DPPC (blue) and DOPC (red). (F) Emission spectra of an equimolar mixture of donor **3** and acceptor **2** in DPPC (blue, solid) and DOPC (red, dashed,  $\lambda_{ex} = 405$  nm, blue arrow in E) with the following controls: Emission spectra of donor **3** (cyan, dashed) and acceptor **2** (blue, dotted) in DPPC, excitation spectrum of acceptor **2** in DPPC (gray, dotted) and DOPC (black, dotted), all at 25 °C.

the first relaxed excited state is fully planarized in all environments, and excluded contributions from solvatochromism. Clearly, the twisted flippers **2** act very differently from ordinary push–pull membrane probes.<sup>1–3</sup>

Double-flipper control **4** with reduced macrodipole gave not only an overall blue-shifted excitation maximum ( $\lambda_{ex} = 498$ – $533$  nm) but also an incomplete planarization in  $S_o$  membranes ( $\lambda_{ex} = 420$  nm observed in  $L_d$  membranes was partially preserved,  $\Delta F_{ex}^1/F_{ex}^2 = 1.1$ , Figure 2C). Nevertheless, the red shift  $\Delta\lambda_{ex} = +66$  nm of **4** in response to planarization remained significant (**2**:  $\Delta\lambda_{ex} = +45$  to  $+80$  nm). All single-flipper controls prepared and tested were useless because of poor partitioning (**6**, Figure S2) or mechanosensitivity (**5**, Figure S3).

Fluorescence depth quenching was used to explore probe repositioning upon membrane reorganization.<sup>18</sup> DPPC vesicles were labeled with DOXYL-PC probes carrying the quencher either in position 5 or 12 of the lipid tails (Figure 1B). Parallax analysis of the different quenching efficiencies of 5- and 12-DOXYL-PC gave  $z_{cf}$  that is the traverse distance  $z$  from the plane of the bilayer center to the plane containing the fluorophore (Figures S8, S9). The  $z_{cf} = 15.1$  Å obtained for **2** exceeded  $z_{cf} = 9.6$  Å of **4** and  $z_{cf} = 1.6$  Å of **3** clearly (Figure 1). Assuming that positioning is determined by external charges and coaxial alignment with the lipid tails (Figure 1),  $z_{cf}$  decreasing with  $2 > 4 > 3$  suggested that quenching occurs preferably near the donor terminus of push–pull fluorophores. Coaxial probe alignment with lipid tails was in agreement with preliminary results from fluorescence anisotropy measurements in GUVs, depth quenching by hole transfer was consistent with the literature.<sup>19</sup> Cooling

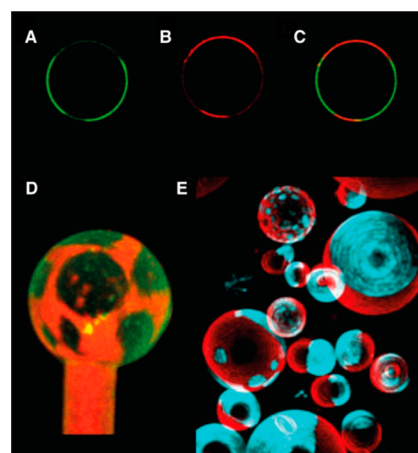


**Figure 3.** Individual (A and B) and merged (C) single-plane CLSM images of the equator region of GUVs composed of SM/DOPC/CL 58:25:17 with 0.1 mol % of **2** obtained by simultaneously recording emission upon excitation at shorter (A,  $\lambda_{ex} = 480$  nm) and longer wavelength (B,  $\lambda_{ex} = 560$  nm). (D) Immobilized on a micropipette, complete GUVs were reconstructed from z-scans in  $0.8$   $\mu\text{m}$ -increments and color coded for emission from excitation at shorter (green) and longer wavelength (red). (E) CLSM images of reconstructed GUVs composed of SM/DOPC/CL 56:24:20 with 0.1 mol % of **2** (red) and 0.01% of ATTO647N (cyan,  $\lambda_{ex} = 630$  nm). The diameters of all shown GUVs were around  $5$ – $10$   $\mu\text{m}$ .

down from  $L_d$  into  $S_o$  DPPC, the  $z_{cf}$  of flipper **2** decreased from  $z_{cf} = 15.1$  Å to  $z_{cf} = 12.3$  Å, i.e.,  $\Delta z_{cf} = -2.8$  Å (**4**,  $\Delta z_{cf} = 0$  Å; **3**,  $\Delta z_{cf} = +2.1$  Å). This very minor probe repositioning upon membrane reorganization is quite remarkable. Mismatched objects are not often tolerated in crystalline  $S_o$  membranes and usually simply ejected.<sup>20</sup> Depth quenching experiments thus provided powerful experimental support that the up to  $\Delta\lambda_{ex} = +80$  nm observed upon  $L_d$  to  $S_o$  phase change originates indeed from planarization of the twisted push–pull mechanophore **2** and not a change in location of the fluorophore.

Fluorescence lifetimes of **2** increased from 2.2 ns in  $L_d$  DOPC LUVs to 4.3 ns in  $S_o$  DPPC LUVs (Figure 2D, circles). Clearly better than those of the flipper-free original **1** (DOPC, 0.47 ns; DPPC, 0.76 ns, Figure 2D, squares), these lifetimes are in the range of established bioprobes,<sup>3a</sup> and thus demonstrate compatibility of fluorescent flippers **2** with FLIM. Preliminary results with GUVs fully support this conclusion. In agreement with the high  $\phi = 83\%$  found in  $\text{CHCl}_3$ , these findings provide corroborative evidence for the validity of the concept of fluorescent flippers.

Partition coefficients measured<sup>21</sup> for flipper **2** indicated a weak preference for  $L_d$  membranes over  $S_o$  membranes at 25 °C (DPPC,  $K_x = 7.7 \times 10^4$ ; DOPC,  $K_x = 1.3 \times 10^5$ , Figure S10). Confocal laser scanning microscopy (CLSM) of GUVs composed of SM/DOPC/CL 58:25:17 (SM: sphingomyelin, CL: cholesterol) and labeled with flipper **2** showed two domains, which light up by exciting at different wavelengths (Figure 3A,  $\lambda_{ex} = 480$  nm, green; Figure 3B,  $\lambda_{ex} = 560$  nm, red; Figure 3C, merged). Co-labeling experiments with a commercial probe for the  $L_d$  phase (cyan,  $\lambda_{ex} = 630$  nm, Figure 3E) confirmed that the emission observed upon excitation at longer wavelength (red,  $\lambda_{ex} = 551$  nm, Figure 3E) arises from flipper **2** in the  $L_o$  phase (red, Figure 3B).

Twisted push–pull flippers report on their environment with shifts of their excitation maxima. Although unproblematic for fluorescence imaging (Figure 3), shifts in emission rather than

excitation are preferable for biological probes. To transcribe shifts in excitation to shifts in emission, terthiophene **3** was considered as FRET donor for mechanophore **2** (Figure 1). Donor **3** exhibited a mechanoinensitive hypsochromic  $\lambda_{\text{ex}} = 400$  nm in DOPC and DPPC membranes (Figure 2E, dashed, cyan and purple). In this region, the excitation of flipper **2** is weak and mechanoinensitive (Figure 2E, dotted, blue, red). Flipper **2** will thus not interfere significantly with the excitation of donor **3** under varied conditions.

The emission maximum of donor **3** at  $\lambda_{\text{em}} = 460$  nm (Figure 2F, dashed, cyan) coincided roughly with the excitation maxima of flipper **2** in DOPC (Figure 2F, dotted, black) and DPPC (Figure 2F, dotted, gray). In DOPC LUVs colabeled with donor **3** and acceptor **2** at equal concentrations, excitation of donor **3** at 405 nm gave an emission spectrum with dominant donor emission at  $\lambda_{\text{em}} = 460$  nm (Figure 2F, dashed, red). In DPPC LUVs under identical conditions, a significant new maximum appeared at  $\lambda_{\text{em}} = 600$  nm (Figure 2F, solid, blue). This difference was consistent with the occurrence of significant FRET to the planarized, more fluorescent flipper **2** in  $S_0$  membranes and negligible FRET to the deplanarized, less fluorescent flipper **2** in  $L_d$  membranes. Control experiments under identical conditions in DPPC with original probe **1** in place of flipper **2** did not afford significant FRET because of insufficient fluorescence of acceptor **1**. These results demonstrate that the transcription of the red shift up to  $\Delta\lambda_{\text{ex}} = +80$  nm achieved by ground-state planarization of push–pull flippers **2** to  $\Delta\lambda_{\text{em}} = +140$  nm in emission is possible with FRET.

Taken together, these results describe the first mechanosensitive push–pull probe that (a) operates, with all likelihood, by planarization of single isolated mechanophores in the ground state (rather than the formation or rearrangement of aggregates) and (b) offers properties that are sufficient for use in practice. This breakthrough was achieved with the introduction of “fluorescent flippers” (large, bright monomers). They provide access to the mechanosensitivity and fluorescence lifetime needed for biological applications (i.e.,  $\Delta\lambda_{\text{ex}}$  up to +80 nm (from ground-state planarization),  $\Delta\lambda_{\text{em}} = +140$  nm (transcribed by FRET),  $\Delta\tau = 2.1$  ns,  $\phi > 80\%$ ). Current efforts focus on the polishing of the operational flippers with regard to twist, macrodipole and terminal charges, on covalent FRET probes, and on applications toward biophysical and biological questions related to membrane order, potential and tension.

## ■ ASSOCIATED CONTENT

### ■ Supporting Information

Detailed experimental procedures. This material is available free of charge via the Internet at <http://pubs.acs.org>.

## ■ AUTHOR INFORMATION

### Corresponding Authors

marta.dal@unige.ch

stefan.matile@unige.ch

### Notes

The authors declare no competing financial interest.

## ■ ACKNOWLEDGMENTS

We thank Giulio Gasparini, David Alonso Doval, Andrea Fin and Nicolas Chiaruttini for contributions to synthesis and experiments, the NMR and the Sciences Mass Spectrometry (SMS) platforms for services, and the University of Geneva, the European Research Council (ERC Advanced Investigator, MGG, SM; Starting Investigator, AR), the National Centre of

Competence in Research (NCCR) Chemical Biology (MGG, SM, AR), the NCCR Molecular Systems Engineering (SM) and the Swiss NSF for financial support (MGG, SM, AR, EV). ED is a fellow of the HFSP.

## ■ REFERENCES

- (1) Baumgart, T.; Hunt, G.; Farkas, E. R.; Webb, W. W.; Feigenson, G. W. *Biochim. Biophys. Acta* **2007**, *1768*, 2182.
- (2) (a) Yan, P.; Xie, A.; Wei, M.; Loew, L. M. *J. Org. Chem.* **2008**, *73*, 6587. (b) Prifti, E.; Reymond, L.; Umehayashi, M.; Hovius, R.; Riezman, H.; Johnsson, K. *ACS Chem. Biol.* **2014**, *3*, 606.
- (3) (a) Wu, Y.; Stefl, M.; Olzynska, A.; Hof, M.; Yahioğlu, G.; Yip, P.; Casey, D. R.; Ces, O.; Hupolickova, J.; Kuimova, M. K. *Phys. Chem. Chem. Phys.* **2013**, *15*, 14986. (b) Dakanali, M.; Do, T. A.; Horn, A.; Chongchivivat, A.; Jarusreni, T.; Lichlyter, D.; Guizzunti, G.; Haidekker, M. A.; Theodorakis, E. A. *Bioorg. Med. Chem.* **2012**, *20*, 4443.
- (4) Zamotaiev, O. M.; Postupalenko, V. Y.; Shvadchak, V. V.; Pivovarenko, V. G.; Klymchenko, A. S.; Mély, Y. *Org. Biomol. Chem.* **2014**, *12*, 7036.
- (5) Rao, M.; Mayor, S. *Biochim. Biophys. Acta* **2005**, *1746*, 221.
- (6) Miller, W.; Lin, J. Y.; Frady, E. P.; Steinbach, P. A.; Kristan, W. B., Jr.; Tsien, R. Y. *Proc. Natl. Acad. Sci. U.S.A.* **2012**, *109*, 2114.
- (7) Bagatolli, L. A. *Biochim. Biophys. Acta* **2006**, *1758*, 1541.
- (8) Reeve, J. E.; Corbett, A. D.; Boczarow, I.; Kaluza, W.; Barford, W.; Bayley, H.; Wilson, T.; Anderson, H. L. *Angew. Chem., Int. Ed.* **2013**, *52*, 9044.
- (9) Stöckl, M. T.; Herrmann, A. *Biochim. Biophys. Acta* **2010**, *1798*, 1444.
- (10) Demchenko, A. P. *J. Fluoresc.* **2010**, *20*, 1099.
- (11) (a) Alonso Doval, D.; Dal Molin, M.; Ward, S.; Fin, A.; Sakai, N.; Matile, S. *Chem. Sci.* **2014**, *5*, 2819. (b) Fin, A.; Vargas-Jentzsch, A.; Sakai, N.; Matile, S. *Angew. Chem., Int. Ed.* **2012**, *51*, 12736.
- (12) (a) Sakai, N.; Matile, S. *J. Am. Chem. Soc.* **2002**, *124*, 1184. (b) Winum, J.-Y.; Matile, S. *J. Am. Chem. Soc.* **1999**, *121*, 7961.
- (13) (a) Wiggins, K. M.; Brantley, J. N.; Bielański, C. W. *Chem. Soc. Rev.* **2013**, *42*, 7130. (b) Ciardelli, F.; Ruggeri, G.; Pucci, A. *Chem. Soc. Rev.* **2013**, *42*, 857. (c) Chi, Z.; Zhang, X.; Xu, B.; Zhou, X.; Ma, C.; Zhang, Y.; Liu, S.; Xu, J. *Chem. Soc. Rev.* **2012**, *41*, 3878. (d) Pawle, R. H.; Haas, T. E.; Müller, P.; Thomas, S. W., III. *Chem. Sci.* **2014**, *5*, 4184. (e) Ho, H.-A.; Najari, A.; Leclerc, M. *Acc. Chem. Res.* **2008**, *41*, 168.
- (14) (a) Diz-Munoz, A.; Fletcher, D. A.; Weiner, O. D. *Trends Cell Biol.* **2013**, *23*, 47. (b) Wang, Y.; Liu, Y.; DeBerg, H. A.; Nomura, T.; Tonks Hoffman, M.; Rohde, P. R.; Schulten, K.; Martinac, B.; Selvin, P. R. *eLife* **2014**, *3*, e01834.
- (15) (a) van Rijn, P.; Janeliunas, D.; Brizard, A. M. A.; Stuart, M. C. A.; Eelkema, R.; van Esch, J. H. *Chem.—Eur. J.* **2010**, *16*, 13417. (b) Effenberger, F.; Würthner, F. *Angew. Chem., Int. Ed.* **1993**, *32*, 719. (c) Nesterov, E. E.; Skoch, J.; Hyman, B. T.; Klunk, W. E.; Bacskai, B. J.; Swager, T. M. *Angew. Chem., Int. Ed.* **2005**, *44*, 5452. (d) Lu, Z.; Liu, N.; Lord, S. J.; Bunge, S. D.; Moerner, W. E.; Twieg, R. J. *Chem. Mater.* **2009**, *21*, 797. (e) Klingstedt, T.; Shirani, H.; Åslund, K. O. A.; Cairns, N. J.; Sigurdson, C. J.; Goedert, M.; Nilsson, K. P. R. *Chem.—Eur. J.* **2013**, *19*, 10179.
- (16) (a) Barbarella, G. *Chem.—Eur. J.* **2002**, *8*, 5072. (b) Palama, I.; Di Maria, F.; Viola, I.; Fabiano, E.; Gigli, G.; Bettini, C.; Barbarella, G. *J. Am. Chem. Soc.* **2011**, *133*, 17777. (c) Santato, C.; Favaretto, L.; Melucci, M.; Zanelli, A.; Gazzano, M.; Monari, M.; Isik, D.; Banville, D.; Bertolazzi, S.; Loranger, S.; Cicoira, F. *J. Mater. Chem.* **2010**, *20*, 669. (d) Kim, O.-K.; Fort, A.; Barzoukas, M.; Blanchard-Desce, M.; Lehn, J.-M. *J. Mater. Chem.* **1999**, *9*, 2227.
- (17) Almeida, P. F. F.; Vaz, W. L. C.; Thompson, T. E. *Biochemistry* **1992**, *31*, 6739.
- (18) Abrams, F. S.; London, E. *Biochemistry* **1992**, *31*, 5312.
- (19) Matko, J.; Ohki, K.; Edidin, M. *Biochemistry* **1992**, *31*, 703.
- (20) Otto, S.; Osifchin, M.; Regen, S. L. *J. Am. Chem. Soc.* **1999**, *121*, 10440.
- (21) White, S. H.; Wimley, W. C.; Ladokhin, A. S.; Hristova, K. *Methods Enzymol.* **1998**, *295*, 62.